Article

Signal-Enhanced Detection of Multiplexed Cardiac Biomarkers by a Paper-Based Fluorogenic Immunodevice Integrated with Zinc Oxide Nanowires

Xueying Guo, Lijun Zong, Yucui Jiao, Yufeng Han, Xiaopan Zhang, Jia Xu, Lin Li, Cheng-wu Zhang, Zhipeng Liu, Qiang Ju, Jinhua Liu, Zhihui Xu, Hai-Dong Yu, and Wei Huang

Anal. Chem., **Just Accepted Manuscript** • DOI: 10.1021/acs.analchem.9b02557 • Publication Date (Web): 17 Jun 2019

Signal-Enhanced Detection of Multiplexed Cardiac Biomarkers by a Paper-Based Fluorogenic Immunodevice Integrated with Zinc Oxide Nanowires

Xueying Guo,[†] Lijun Zong,[†] Yucui Jiao,[†] Yufeng Han,[†] Xiaopan Zhang,[†] Jia Xu,[†] Lin Li,[†] Cheng-wu Zhang,[†] Zhipeng Liu,[†] Qiang Ju,[†] Jinhua Liu,[*,†] Zhihui Xu,[*,§] Hai-Dong Yu,[*,†,‡] and Wei Huang[*,†,‡]

[†] Institute of Advanced Materials (IAM) & Key Laboratory of Flexible Electronics (KLOFE), Jiangsu National Synergetic Innovation Center for Advanced Materials (SICAM), Nanjing Tech University (NanjingTech), 30 South Puzhu Road, Nanjing 211816, PR China

[‡]Xi'an Institute of Flexible Electronics, Northwestern Polytechnical University, 127 West Youyi Road, Xi'an 710072, PR China

[§]Department of Cardiology, The First Affiliated Hospital of Nanjing Medical University, 300 Guangzhou Road, Nanjing 210029, PR China

ABSTRACT: Using a single test to comprehensively evaluate multiple cardiac biomarkers for early diagnosis and prevention of acute myocardial infarction (AMI) has been facing enormous challenges. Here, we have developed paper-based fluorogenic immunodevices for multiplexed detection of three cardiac biomarkers, namely, human heart-type fatty acid-binding protein (FABP), cardiac troponin I (cTnI), and myoglobin, simultaneously. The detection is based on a strategy using zinc oxide nanowires (ZnO NWs) to enhance fluorescence signals (~5-fold compared to that on pure paper). The immunodevices showed high sensitivity and selectivity for FABP, cTnI, and myoglobin with detection limits of 1.36 ng/mL, 1.00 ng/mL, and 2.38 ng/mL, respectively. Additionally, the paper-based immunoassay was rapid (~5 minutes to complete the test) and portable (using a homemade chamber with a smartphone and an ultraviolet lamp). The developed devices integrated with ZnO NWs enable quantitative, sensitive, and simultaneous detection of multiple cardiac biomarkers in point-of-care settings, which provides a useful approach for monitoring AMI diseases and may be extended to other medical diagnostics and environmental assessments.

As one of the clinical forms of coronary syndromes, acute myocardial infarction (AMI) is one of the most common causes of death.[1] When AMI occurs, the concentration of biomarkers in blood for myocardial injury increase sharply, such as human heart-type fatty acid-binding protein (FABP), cardiac troponin I (cTnI), and myoglobin.[2-4] It is often necessary to simultaneously detect several biomarkers to produce meaningful or conclusive information, which ensures an accurate diagnosis and reduced patient risk.[5] Current techniques for monitoring AMI include ELISA, electrochemiluminescence, and surface plasmon resonance.[6-8] These tests can only be performed in hospitals or specialized diagnostic centers and require professional operation and bulky instrumentation, which prevents many people from getting a timely diagnosis. These tests also cannot detect several cardiac biomarkers simultaneously. Until now, comprehensive evaluation of multiple cardiac biomarkers by a single test has been limited.

Paper-based analytical devices have the potential to overcome many of the above drawbacks because they are 1) inexpensive, printable, and easy to manufacture;[9,10] 2) lightweight and portable; and 3) biocompatible, eco-friendly, and disposable.[11-14] The three-dimensional network structure of the paper allows capillary-driven flow without external power or equipment (e.g., pumps) when directly contacting liquids. The fabrication techniques of paper-based analytical devices include surface polymerization,[15] photolithography,[16] the drawing method,[17] calendaring,[18] wax printing,[19,20] and so on. Among them, wax printing is simple, rapid, inexpensive, and efficient for large-scale production of paper-based analytical devices. Paper-based devices have gained enormous interest since Whitesides' group introduced a promising concept of using a patterned paper substrate as a microfluidic platform for simultaneous detection of multiple analytes.[21,22] For example, Qi et al. have designed a microfluidic paper-based device with CdTe quantum dots for fluorescence detection of Cu^{2+} and Hg^{2+} ions;[23] Martinez et al. have introduced a paper-based device for colorimetric testing of glucose and protein;[16] and Deraney et al. have developed a paper-based device for colorimetric diagnosis of malaria and dengue fever.[24] Among various detection methods of paper-based assays, paper-based fluorescence immunoassays have been applied in chemical and biological detection due to rapid detection, high sensitivity and selectivity, and user-friendly operation.[25-29] However, most current fluorescence immunoassays require specialized fluorescence readers such as a fluorescence spectrometer, fluorescence microscope and so on. The problems of autofluorescence and high scattering still exist when performing analyses on paper and reduce the signal-to-background ratios and hamper the practical application of paper-based fluorescence assays.[30,31]

Integration of various nanomaterials in diagnostic devices may greatly improve their performance,[32,33] e.g., nanoscale zinc oxide (ZnO) exhibits excellent piezoelectric performance, good biocompatibility, etc.[34,35] Recently, it has been reported that zinc oxide nanowires (ZnO NWs) can enhance the fluorescence intensity in various biomedical assays, allowing high-throughput detection of proteins.[36,37] For instance, Guo et al. have developed microfluidic chips integrated with ZnO NWs for the detection of cancer biomarkers, achieving a superior limit of detection as low as 1 pg/mL in the human α-fetoprotein assay and 100 fg/mL in the carcinoembryonic antigen assay.[38] On the other hand, specialized fluorescence readers for fluorescence detection can be replaced by mobile phones, which are ubiquitous and easy to use in modern society. For example, Martinez et al. have reported that low-cost mobile phones are suitable for chromophoric paper-based assays, which sensitively capture the output of assays.[39] Other groups have also shown that mobile phones (including smartphones) can be used as imaging tools for chromophore- and fluorophore-labeled (including paper-based) assays.[40]

In this work, we have developed a paper-based fluorogenic immunodevice for the quantitative and multiplexed detection of three cardiac biomarkers, FABP, cTnI, and myoglobin. ZnO NWs were integrated with the paper-based devices using a simple hydrothermal method, which can enhance the fluorescence intensity significantly. The detection limits for FABP, cTnI, and myoglobin were 1.36 ng/mL, 1.00 ng/mL, and 2.38 ng/mL, respectively. A homemade chamber including a smartphone and an ultraviolet lamp was used for paper-based detection, suggesting the portability of this method. This work provides a simple, low-cost, portable, and robust diagnostic test of multiple cardiac biomarkers, which holds great potential in clinical diagnosis, food safety, environmental monitoring, and so on.

EXPERIMENTAL SECTION

Chemicals and materials. Whatman No. 1 chromatography paper was purchased from Shanghai Zhengcheng Experimental Instrument Co., Ltd. Zinc acetate dehydrate, zinc nitrate hexahydrate, polyethyleneimine, (3-glycidyloxypropyl)trimethoxysilane, and hexamethylenetetramine (99%) were purchased from Shanghai Titanchem Co., Ltd. Methoxy polyethylene glycol thiol was purchased from Shanghai Yuanye Biological Technology Co., Ltd. Human heart-type fatty acid-binding protein (FABP), cardiac troponin I (cTnI), myoglobin, capture monoclonal antibodies (anti-FABP, anti-cTnI, and anti-myoglobin), and FITC-labeled antibodies (anti-FABP, anti-cTnI, and anti-myoglobin) were purchased from Shanghai Linc-Bio Science Co., Ltd. Human serum, rabbit immunoglobulin G (IgG), and FITC-labeled goat anti-rabbit IgG were purchased from Beijing Biodragon Immunotechnologies Co., Ltd. Ammonium hydroxide (28%) was purchased from Shanghai Lingfeng Chemical Reagent Co., Ltd. Tween-20, bovine serum albumin, and ethanol (99.5%) were purchased from Shanghai Macklin Biochemical Co., Ltd. Phosphate buffered saline (PBS, 0.01 mol/L, pH = 7.4) and phosphate buffer saline solution containing 0.05% Tween-20 (PBST) were freshly prepared. Red ink was purchased from Nanjing WanQing Chemistry Glass Instrument Co., Ltd. Three commercialized ELISA kits for the respective detection of FABP, cTnI, and myoglobin were purchased from Shanghai Enzyme-linked Biotechnology Co., Ltd. Blotting paper was purchased from Zhengzhou, Henan Ruikang raw reagent stores. All chemicals used in experiments were of analytical grade without further purification. Ultrapure water (18.2 MΩ • cm at 25 ºC) was obtained from a Milli-Q system (Millipore, Bedford, MA, USA).

Instruments. The morphology of zinc oxide nanowires (ZnO NWs) was acquired with a field-emission scanning electron microscope (SEM, JEOL JSM-6701F). X-ray diffraction (XRD, Rigaku, Ultima III) patterns were collected using Cu Kα radiation (45 kV, 40 mA) from 10° to 60°. Energy dispersive spectroscopy (EDS) was used for analyzing the molecular composition. The images captured by the smartphone camera (Mi Note3) were transferred to a computer for further analysis using the image processing software ImageJ. A portable, battery-powered ultraviolet lamp with emission at 365 nm was purchased at Beijing Tianmai Henghui Light Source Electric Co., Ltd. Fluorescence spectra were obtained in a microplate reader (Cytation5, BIOTEK). The paper-based devices were printed using a spray wax printer (ColorQube 8580 N, Xerox, USA).

Synthesis of ZnO NWs on paper. ZnO NWs were prepared on Whatman No. 1 chromatography paper via a modified hydrothermal method.[38,41] The paper was immersed in a solution of zinc acetate dihydrate (2.19 g/100 mL water) for 1 min. The wet paper was dried at

100 °C for 1 h. The paper was then dipped into a solution containing 0.372 mol/L ammonia hydroxide, 25 mmol/L zinc nitrate hexahydrate, 12.5 mmol/L hexamethylenetetramine, and 5 mmol/L polyethyleneimine and heated in an oven at 90 °C for 3 h. The obtained ZnO NW/paper was washed with water three times and dried for further use.

Fabrication of the paper-based immunodevice. The ZnO NW/paper was used to fabricate paper-based devices (Figures S1A and B). The patterns designed by Microsoft PowerPoint were printed on ZnO NW/paper using a spray wax printer. The ZnO NW/paper was then placed in an oven at 120 °C for 2 min. The immunodevice was divided into layer A and layer B, where layer A contained detection zones with diameters of 3.5 mm. The surfaces of ZnO NWs on detection zones were modified with 4% (3-glycidyloxypropyl)trimethoxysilane (GPTMS) in ethanol for 20 min to acquire the epoxy groups that can effectively immobilize capture antibodies. Then, 2.5 μL of 60 μg/mL capture antibody solutions of anti-FABP, anti-cTnI, and anti-myoglobin were dropped into corresponding detection zones and incubated for 30 min under ambient conditions. Unreacted epoxy groups on the surface of ZnO NWs were blocked using 1% methoxy polyethylene glycol thiol and 1% bovine serum albumin (BSA). Finally, the immunodevices were stored at 4 °C for further use.

Detection of cardiac biomarkers. Cardiac biomarkers were detected based on a sandwich immunoassay on paper-based immunodevices (Figure 4). Layer B was folded on top of layer A using simple origami principles. First, 15 μL of sample solution containing different concentrations of FABP, cTnI, and myoglobin in an incubation buffer (0.05% Tween-20 in PBS) was added to the central sample zone of layer B, which then flowed to the detection zones on layer A. After drying for 1 min under ambient conditions, 2.5 μL of 80 μg/mL FITC-labeled anti-FABP, FITC-labeled anti-cTnI, and FITC-labeled anti-myoglobin were added to the corresponding detection zones. After a 1-min incubation under ambient conditions, each detection zone was washed three times by adding 10 μL of PBST to the zone, bringing the bottom of the paper-based immunodevice in contact with a piece of blotting paper to absorb the excess solution. Finally, the paper-based devices were placed in a homemade chamber using a battery-powered UV lamp for excitation and a smartphone for capturing the fluorescence images. It took approximately 5 minutes to complete the test with the prepared immunodevice. For semiquantitative testing, the results could be directly read by the naked eye. All experiments were performed seven times to ensure reproducibility. For real sample analysis, blood samples were collected from 15 AMI patients at the First Affiliated Hospital of Nanjing Medical University. The sera (from centrifuged raw human blood) were diluted with PBS buffer (pH = 7.4). Three commercialized ELISA kits were also used for detecting FABP, cTnI, and myoglobin in the clinical samples to compare with results obtained from our paper-based method.

Data analysis. The fluorescence images captured by the smartphone camera were transferred to a computer for further analysis using the image processing software ImageJ. An average green channel value was obtained for each detection zone by selecting the whole area of each zone. The average green channel values of the blank samples were used as background and subtracted from the value of the detection zone.

RESULTS AND DISCUSSION

Design and fabrication of paper-based devices. A foldable paper-based device for fluorescence immunoassay was designed and fabricated by a wax printing technique,[19] as illustrated in Figures 1B and S1A. Considering the detection of multiple biomarkers from a single sample using only one device, the device comprises one application zone that directs the sample to all other channels within the device, which allows minimum manipulation of the sample and ensures uniform distribution of the sample volume between all fluidic pathways within the device. The detection zones for multiple biomarkers were located on a common layer to perform assays, which is simultaneously convenient for signal output. Based on this, the paper-based device was designed to consist of two layers, layers A and B, that could be folded (Figure S1A). Layer A is the detection layer, including three detection zones for detection of three cardiac biomarkers. Layer B is the sample layer. One sample zone is at the center, where the sample is added to the central zone and shunted to three detection zones. When layer B is folded over layer A, the sample will flow to corresponding detection zones on layer A. The corresponding FITC-labeled antibodies were added to three detection zones on layer A, and fluorescence images were captured by a smartphone (Figure 1B).

Characterization of ZnO NWs grown on paper. We have integrated ZnO NWs on paper-based devices through a hydrothermal method. From SEM images of pure paper, we observed a network of bare cellulose fibers (Figures 2A and B). As shown in the SEM images of ZnO NW/paper, dense arrays of well-aligned ZnO NWs were vertically grown on the cellulose fibers of paper with full surface coverage (Figures 2C and D). The EDS spectrum of ZnO NW/paper shows clear peaks of Zn and O (Figure 2E), which also indicates successful preparation of ZnO NWs on paper. The XRD pattern of pure paper reveals three peaks at 2θ = 14.7°, 16.8°, and 22.7° (Figure 2F), which correspond to the planes of crystallinity of cellulose forming the fibers of the paper. In addition to these three peaks, the XRD pattern of ZnO NW/paper reveals five more peaks at 2θ = 31.7°, 34.4°, 36.3°, 47.5°, and 56.6° (Figure 2F), which correspond to the (100), (002), (101), (102), and (110) planes of ZnO, respectively. The characteristic peaks of ZnO NWs agree with the standard ZnO XRD pattern, and the diffraction patterns contain no impurity peaks, implying the high purity of the ZnO NWs grown on paper.

Signal enhancement by ZnO NWs on paper. To evaluate the fluorescence enhancement ability of ZnO NWs, the fluorescence intensity of FITC-labeled IgG was tested, while PBS was tested as a control. As shown in Figure 3a and c, there was no significant difference in the fluorescence intensity of PBS on paper and ZnO NW/paper, suggesting that the background signal was similar. The fluorescence intensity of FITC-labeled IgG was higher than that of PBS on both paper and ZnO NW/paper. However, the fluorescence intensity of FITC-labeled IgG on ZnO NW/paper was ~5-fold higher than that on paper (Figure 3b and d). This value is similar but slightly lower than that on rigid glass substrates modified with ZnO.[36,42] This result indicated that the ZnO NW/paper enables signal enhancement of fluorescence intensity, which provides a better device for fluorescence detection by improving the signal-to-noise ratio and the overall sensitivity. It has been reported that fluorescence can be enhanced by ZnO NWs because of their large surface-to-volume ratio, aspect ratio, and intrinsic fluorescence enhancement properties.[43]

Portable detection of cardiac biomarkers. The paper-based detection of rabbit IgG was performed in a homemade chamber using a battery-powered UV lamp for excitation and a smartphone for capturing the fluorescence images (Figure 4A), suggesting the portability of this method. The portable approach has been further used for the multiplexed detection of cardiac biomarkers in PBS and human serum, where a sandwich immunoassay was performed on a paper-based device (Figure 4B): (1) The capture antibodies for FABP, cTnI, and myoglobin were preimmobilized in three detection zones for simultaneous detection of these cardiac biomarkers, while 1% BSA was used for blocking the

nonspecific binding sites. (2) The sample solution containing cardiac biomarkers was added to the central sample zone and shunted to three detection zones. (3) The cardiac biomarkers were specifically bound to the respective capture antibody. (4) The cardiac biomarkers were sandwiched between capture antibodies and FITC-labeled antibodies, which were specifically bound to different recognition sites of the cardiac biomarkers. As the entire assay was performed without relying on any dedicated instrument, this portable device can be widely used in point-of-care settings.

Multiplexed detection of cardiac biomarkers in PBS. Excellent high throughput fluorescence immunoassays must exclude interference. To determine whether there was any interference in the signal generation with multiple analytes in the paper-based device, 15 μL of PBS containing various combinations of three cardiac biomarkers, that is, FABP, cTnI, and myoglobin, was added to the sample zone. When 50 ng/mL FABP was present in the sample, only the detection zone for FABP was developed (Figure S11B). In the case of 50 ng/mL cTnI, only the detection zone for cTnI was developed (Figure S11C). In the case of 50 ng/mL myoglobin, only the detection zone for myoglobin was developed (Figure S11D). Obviously, the cross-reactivity between analytes and noncognate antibodies was negligible. Simultaneous detection of three cardiac biomarkers was demonstrated in this paper-based device by dropping 15 μL of PBS containing FABP (50 ng/mL), cTnI (50 ng/mL), and myoglobin (50 ng/mL) into the sample zone. In this case, all three detection zones were developed in their respective detection zones (Figure S11H). For these experiments, we also assessed all possible combinations of three cardiac biomarkers: all positive, all negative, and combinations of FABP, cTnI, and myoglobin (Figure S11). Additional samples that contained at least one antigen (i.e., positive for either one, two, or three cardiac biomarkers) had a strong positive fluorescence signal for positive immunoassays (Figures S11B-H). Thus, simultaneous detection of multiple cardiac biomarkers could be performed on this designed paper-based fluorogenic immunodevice.

Quantitative detection of cardiac biomarkers in PBS. We have investigated the analytical performance of this paper-based device integrated with ZnO NWs for the detection of samples containing FABP, cTnI, and myoglobin at various concentrations. The calibration curves for three cardiac biomarkers are shown in Figure 5. With increasing concentrations of FABP, cTnI, and myoglobin, the green channel intensity value responses increased gradually. The green channel intensity value responses increased linearly with increasing concentrations of FABP over the range of 2.5-60 ng/mL (Figure 5A). The linear regression equation was $y = 0.88x + 5.34$ ($R^2 = 0.98$), where y is the green channel intensity value with the blank control subtracted and x is the concentration of cardiac biomarker. The green channel intensity value responses increased linearly with increasing concentration of cTnI over the range of 1-50 ng/mL (Figure 5B). The linear regression equation was $y = 0.90x + 5.87$ ($R^2 = 0.97$). The green channel intensity value responses increased linearly with increasing concentrations of myoglobin over the range of 5-60 ng/mL (Figure 5C). The linear regression equation was $y = 1.01x + 30.15$ ($R^2 = 0.97$). The limits of detection for FABP, cTnI, and myoglobin on ZnO NW/paper were calculated to be 1.36 ng/mL, 1.00 ng/mL, and 2.38 ng/mL, respectively.[44] The results suggest that the paper-based assay was highly sensitive and useful for simultaneously detecting the three cardiac biomarkers. Thus, in view of these calibration curves, the paper-based fluorogenic immunodevice should be helpful for measuring the three cardiac markers in real serum samples, as the cutoff values of the FABP, cTnI, and myoglobin in clinical diagnosis are 2 ng/mL, 1-3 ng/mL, and 15-30 ng/mL, respectively.[45,46] We also studied the detection of FABP, cTnI, and myoglobin on paper (Figure S12). The limits of detection for FABP, cTnI, and myoglobin on paper were estimated as 4.96 ng/mL, 8.23 ng/mL, and 7.94 ng/mL, respectively. Based on the above results, the limits of detection on ZnO NW/paper were improved up to ~8-fold compared to those on paper. It is obvious that the paper-based fluorogenic immunodevice integrated with ZnO NWs greatly improves the sensitivity for detecting cardiac biomarkers, making it within the range of clinically relevant concentrations.

Determination of cardiac biomarkers in human serum. It is important to validate that the paper-based fluorogenic immunodevice enables detection of cardiac biomarkers in real biological samples. The determination of the FABP, cTnI, and myoglobin concentrations in real human serum was conducted using this device. We purchased human serum from a commercial source, and it was used after diluting 100 times with PBS. Different amounts of FABP, cTnI, and myoglobin were spiked into the diluted human serum samples to perform the recovery tests. We obtained the recovery rate in percentage by dividing the amounts of cardiac biomarkers calculated from the measured green channel signal and the calibration curves by the amount of three cardiac biomarkers spiked into the samples. The recoveries for the spiked FABP, cTnI, and myoglobin were 99.7-103%, 96-102%, and 100.1-100.4%, respectively (Table 1). These values are consistent with the accuracy required for trace analysis of complex matrix samples. The results suggest that the paper-based fluorogenic immunodevice integrated with ZnO NWs exhibits high reproducibility and has the potential to become an alternative method for the detection of cardiac biomarkers in clinical samples.

Determination of cardiac biomarkers in clinical samples. We have also studied the performance of the paper-based device integrated with ZnO NWs for detection of biomarkers in clinical samples. Blood samples were collected from 15 AMI patients at the First Affiliated Hospital of Nanjing Medical University. The sera (from centrifuged raw human blood) were diluted with PBS buffer (pH = 7.4). We examined these clinical samples using our paper-based method and compared the results with those obtained by commercialized ELISA kits (Table S2). To analyze the linear dependence between the two methods, Passing-Boblok regression and Spearman's rank correlation coefficients were adopted. Both the slopes of the three regression equations and the Spearman's coefficients were close to 1 (Figure 6). This indicates that the two methods for detection of FABP, cTnI, and myoglobin possessed good linear correlation, which means that the results obtained by our method were comparable to those obtained by commercialized ELISA kits. While the commercialized ELISA kits require expensive instrumentation for detection and a commercialized ELISA kit can only detect one cardiac biomarker, our paper-based method is low-cost and easy to use and only requires a smartphone and an ultraviolet lamp. Simultaneous detection of three cardiac biomarkers can be achieved by a single paper-based fluorogenic immunodevice. Moreover, the paper-based method can detect the clinical samples more quickly (~5 minutes) than the ELISA kits, which took more than 75 minutes to complete. The results indicate that the developed paper-based fluorogenic immunodevice can be practically used for the multiplexed determination of FABP, cTnI, and myoglobin during clinical diagnosis. Moreover, an overview on recently reported methods for determination of cardiac biomarkers is provided in Table S3. In comparison to other methods, the developed paper-based fluorogenic immunodevice has a shorter detection time and higher sensitivity and does not require costly instrumentation.

Paper-based analytical devices may reduce the global disease burden due to their low cost. However, there still remain many challenges before they become widely used products, for example: i) Paper-based devices were studied only in the laboratory, and most devices never leave the

laboratory due to the difficulty of converting a concept in the laboratory to a product in the hands of users.[47,48] ii) Improved stability of paper-based devices related to reagent storage is required, which will be suitable for use in remote locations.[49] iii) Noninvasive approaches based on paper-based devices are expected to eliminate the pain and risk of infections for blood analysis.[50] In this work, sensitivity, one of the key challenges of paper-based analytical devices has been greatly enhanced to meet the standards of clinically relevant concentrations.

CONCLUSION

In summary, we have designed and fabricated a paper-based fluorogenic immunodevice that can be used for portable detection of multiple cardiac biomarkers, namely, FABP, cTnI, and myoglobin, simultaneously. We have integrated this paper-based device with ZnO NWs that have significant fluorescence amplification capability, enabling highly sensitive detection within the range of clinically relevant concentrations. The prominent advantages of this approach include the following: i) Multiplexing: the developed device enables simultaneous detection of three cardiac biomarkers, FABP, cTnI, and myoglobin. ii) Portability: paper-based fluorescence detection was performed in a homemade chamber using a battery-powered UV lamp for excitation and a smartphone for capturing the fluorescence images. Paper-based devices can move fluids by capillary action and require no external power or pumps. iii) Rapid detection: it takes only ~5 minutes to complete the test. Short analysis time is crucial for life, which can reduce mortality. vi) High sensitivity: the limits of detection for FABP, cTnI, and myoglobin on paper were 4.96 ng/mL, 8.23 ng/mL, and 7.94 ng/mL, respectively, whereas the limits of detection on ZnO NW/paper were as low as 1.36 ng/mL for FABP, 1.00 ng/mL for cTnI, and 2.38 ng/mL for myoglobin. The paper-based strategy has great value in clinical, environmental, and biodefense applications thanks to the accurate quantitative analysis of multiple analytes.

ASSOCIATED CONTENT

Supporting Information

The Supporting Information is available free of charge on the ACS Publications website.

AUTHOR INFORMATION

Corresponding Author

***** E-mail: iamhdyu@njtech.edu.cn; iamjhliu@njtech.edu.cn; wx-xzm@163.com; iamwhuang@njtech.edu.cn

Notes

The authors declare no competing financial interest.

ACKNOWLEDGMENT

This work was financially supported by the National Natural Science Foundation of China (21675085, 81672508, 61505077, 21505072), National Key R&D Program of China (2017YFA0204700), China-Sweden Joint Mobility Project (51811530018), Fundamental Studies of Perovskite Solar Cells (2015CB932200), Primary Research & Development Plan of Jiangsu Province (BE2016770), Natural Science Foundation of Jiangsu Province for Distinguished Young Scholars (BK20170042, BK20170041), and Key University Science Research Project of Jiangsu Province (16KJA180004).

REFERENCES

(1) Grabowska, I.; Sharma, N.; Vasilescu, A.; Iancu, M.; Badea, G.; Boukherroub, R.; Ogale, S.; Szunerits, S. *Acs Omega* **2018**, *3*, 12010-12018.

(2) Sonawane, M. D.; Nimse, S. B.; Song, K. S.; Kim, T. *Anal. Methods* **2017**, *9*, 3773-3776.

(3) Sarangadharan, I.; Wang, S. L.; Sukesan, R.; Chen, P. C.; Dai, T. Y.; Pulikkathodi, A. K.; Hsu, C. P.; Chiang, H. H. K.; Liu, L. Y. M.; Wang, Y. L. *Anal. Chem.* **2018**, *90*, 2867-2874.

(4) Zhang, D.; Huang, L.; Liu, B.; Ni, H. B.; Sun, L. D.; Su, E. B.; Chen, H. Y.; Gu, Z. Z.; Zhao, X. W. *Biosens. Bioelectron.* **2018**, *106*, 204-211.

(5) Zhu, J. M.; Zou, N. L.; Zhu, D. N.; Wang, J.; Jin, Q. H.; Zhao, J. L.; Mao, H. J. *Clin. Chem.* **2011**, *57*, 1732-1738.

(6) Pawula, M.; Altintas, Z.; Tothill, I. E. *Talanta* **2016**, *146*, 823-830.

(7) Zhang, L.; Xiong, C. Y.; Wang, H. J.; Yuan, R.; Chai, Y. Q. *Sens. Actuators B: Chem.* **2017**, *241*, 765-772.

(8) Yang, Q. L.; Cai, R. T.; Xiao, W.; Wu, Z. F.; Liu, X.; Xu, Y.; Xu, M. M.; Zhong, H.; Sun, G. D.; Liu, Q. H.; Fu, Q. Q.; Xiang, J. J. *Nanoscale Res. Lett.* **2018**, *13*, 397.

(9) Fratzl, M.; Chang, B. S.; Oyola-Reynoso, S.; Blaire, G.; Delshadi, S.; Devillers, T.; Ward, T.; Dempsey, N. M.; Bloch, J. F.; Thuo, M. M. *Acs Omega* **2018**, 3, 2049-2057.

(10) Oyola-Reynoso, S.; Heim, A. P.; Halbertsma-Black, J.; Zhao, C.; Tevis, I. D.; Cinar, S.; Cademartiri, R.; Liu, X. Y.; Bloch, J. F.; Thuo, M. M. *Talanta* **2015**, 144, 289-293.

(11) Pollock, N. R.; Rolland, J. P.; Kumar, S.; Beattie, P. D.; Jain, S.; Noubary, F.; Wong, V. L.; Pohlmann, R. A.; Ryan, U. S.; Whitesides, G. M. *Sci. Transl. Med.* **2012**, *4*. 152 ra 129.

(12) Ahn, H.; Batule, B. S.; Seok, Y.; Kim, M. G. *Anal. Chem.* **2018**, *90*, 10211-10216.

(13) Tenda, K.; van Gerven, B.; Arts, R.; Hiruta, Y.; Merkx, M.; Citterio, D. *Angew. Chem., Int. Ed.* **2018**, *57*, 15369-15373.

(14) Wu, M. R.; Lai, Q. Y.; Ju, Q.; Li, L.; Yu, H. D.; Huang, W. *Biosens. Bioelectron.* **2018**, *102*, 256-266.

(15) Oyola-Reynoso, S.; Tevis, I. D.; Chen, J.; Chang, B. S.; Cinar, S.; Bloch, J. F.; Thuo, M. M. *J. Mater. Chem. A* **2016**, 4, 14729-14738.

(16) Martinez, A. W.; Phillips, S. T.; Butte, M. J.; Whitesides, G. M. *Angew. Chem., Int. Ed.* **2007**, 46, 1318-1320.

(17) Oyola-Reynoso, S.; Heim, A. P.; Halbertsma-Black, J.; Zhao, C.; Tevis, I. D.; Cinar, S.; Cademartiri, R.; Liu, X. Y.; Bloch, J. F.; Thuo, M. M. *Talanta* **2015**, 145, 73-77.

(18) Oyola-Reynoso, S.; Frankiewicz, C.; Chang, B.; Chen, J.; Bloch, J. F.; Thuo, M. M. *Biomicrofluidics* **2017**, 11, 014104.

(19) Carrilho, E.; Martinez, A. W.; Whitesides, G. M. *Anal. Chem.* **2009**, 81, 7091-7095.

(20) Lu, Y.; Shi, W. W.; Qin, J. H.; Lin, B. C. *Anal. Chem.* **2010**, 82, 329-335.

(21) Martinez, A. W.; Phillips, S. T.; Whitesides, G. M. *Proc. Natl. Acad. Sci. U. S. A.* **2008**, *105*, 19606-19611.

(22) Cheng, C. M.; Martinez, A. W.; Gong, J.; Mace, C. R.; Phillips, S. T.; Carrilho, E.; Mirica, K. A.; Whitesides, G. M. *Angew. Chem., Int. Ed. Engl.* **2010**, *49*, 4771-4774.

(23) Qi, J.; Li, B. W.; Wang, X. R.; Zhang, Z.; Wang, Z.; Han, J. L.; Chen, L. X. *Sens. Actuators B: Chem.* **2017**, *251*, 224-233.

(24) Deraney, R. N.; Mace, C. R.; Rolland, J. P.; Schonhorn, J. E. *Anal. Chem.* **2016**, *88*, 6161-6165.

(25) Zong, L. J.; Jiao, Y. C.; Guo, X. Y.; Zhu, C. X.; Gao, L.; Han, Y. F.; Li, L.; Zhang, C. W.; Liu, Z. P.; Liu, J. H.; Ju, Q.; Yu, H.-D.; Huang, W. *Talanta* **2019**, *195*, 333-338.

(26) Wang, P. L.; Wang, Z.; Su, X. O. *Biosens. Bioelectron.* **2015**, *64*, 511-516.

(27) Lou, D. D.; Fan, L.; Cui, Y.; Zhu, Y. F.; Gu, N.; Zhang, Y. *Anal. Chem.* **2018**, *90*, 6502-6508.

(28) Yang, Q. H.; Gong, X. Q.; Song, T.; Yang, J. M.; Zhu, S. J.; Li, Y. H.; Cui, Y.; Li, Y. X.; Zhang, B. B.; Chang, J. *Biosens. Bioelectron.* **2011**, 30, 145-150.

(29) Chen, Y. Q.; Chen, Q.; Han, M. M.; Liu, J. Y.; Zhao, P.; He, L. D.; Zhang, Y.; Niu, Y. M.; Yang, W. J.; Zhang, L. Y. *Biosens. Bioelectron.* **2016**, 79, 430-434.

(30) Shah, K. G.; Yager, P. *Anal. Chem.* **2017**, *89*, 12023-12029.
(31) Shah, K. G.; Singh, V.; Kauffman, P. C.; Abe, K.; Yager, P. *Anal. Chem.* **2018**, *90*, 6967-6974.
(32) Li, X.; Zhao, C.; Liu, X. Y. *Microsyst. Nanoeng.* **2015**, 1, 15014.
(33) Fu, G. L.; Sanjay, S. T.; Li, X. J. Analyst **2016**, 141, 3883-3889.
(34) Li, X.; Wang, Y. H.; Zhao, C.; Liu, X. Y. *ACS Appl. Mater. Interfaces* **2014**, 6, 22004-22012.
(35) Li, X.; Wang, Y. H.; Lu, A. A.; Liu, X. Y. *IEEE Sens. J.* **2015**, 15, 6100-6107.
(36) Hu, W. H.; Liu, Y. S.; Yang, H. B.; Zhou, X. Q.; Li, C. M. *Biosens. Bioelectron.* **2011**, 26, 3683-3687.
(37) Yu, X.; Xia, Y.; Tang, Y.; Zhang, W. L.; Yeh, Y. T.; Lu, H.; Zheng, S. Y. *Small* **2017**, *13*, 1700425.
(38) Guo, L.; Shi, Y.; Liu, X.; Han, Z.; Zhao, Z.; Chen, Y.; Xie, W.; Li, X. *Biosens. Bioelectron.* **2018**, *99*, 368-374.
(39) Martinez, A. W.; Phillips, S. T.; Carrilho, E.; Thomas, S. W.; Sindi, H.; Whitesides, G. M. *Anal. Chem.* **2008**, *80*, 3699-3707.
(40) Vashist, S. K.; Mudanyali, O.; Schneider, E. M.; Zengerle, R.; Ozcan, A. *Anal. Bioanal. Chem.* **2014**, *406*, 3263-3277.
(41) Tiwari, S.; Vinchurkar, M.; Rao, V. R.; Garnier, G. *Sci. Rep.* **2017**, *7*, 43905.
(42) Wu, Z. H.; Zhao, D.; Hou, C. Y.; Liu, L.; Chen, J. H.; Huang, H.; Zhang, Q. H.; Duan, Y. R.; Li, Y. G.; Wang, H. Z. *Nanoscale* **2018**, 10, 17663-17670.
(43) Sang, C. H.; Chou, S. J.; Pan, F. M.; Sheu, J. T. *Biosens. Bioelectron.* **2016**, *75*, 285-292.
(44) Gong, X. Q.; Zhang, B.; Piao, J. F.; Zhao, Q.; Gao, W. C.; Peng, W. P.; Kang, Q.; Zhou, D. M.; Shu, G. M.; Chang, J. *Nanomedicine* **2018**, *14*, 1257-1266.
(45) Nair, G. V.; Gurbel, P. A.; Fuzaylov, S. Y.; Davis, C. J.; Ohman, E. M.; Bahr, R. D.; Christensen, R. H.; Serebruany, V. L. *Cardiology* **2000**, *93*, 50-55.
(46) Masson, J. F.; Obando, L.; Beaudoin, S.; Booksh, K. *Talanta* **2004**, *62*, 865-870.
(47) Kimani, F. W.; Mwangi, S. M.; Kwasa, B. J.; Kusow, A. M.; Ngugi, B. K.; Chen, J. H.; Liu, X. Y.; Cademartiri, R.; Thuo, M. M. *Micromachines* **2017**, 8, 317.
(48) Kumar, A. A.; Hennek, J. W.; Smith, B. S.; Kumar, S.; Beattie, P.; Jain, S.; Rolland, J. P.; Stossel, T. P.; Chunda-Liyoka, C.; Whitesides, G. M. *Angew. Chem., Int. Ed.***2015**, 54, 5835-5852.
(49) Tian, T.; Bi, Y. P.; Xu, X.; Zhu, Z.; Yang, C. Y. *Anal. Methods* **2018**, 10, 3567-3581.
(50) Liu, Q.; Wang, J. H.; Wang, B. K.; Li, Z.; Huang, H.; Li, C. Z.; Yu, X. F.; Chu, P. K. *Biosens. Bioelectron.* **2014**, 54, 128-134.

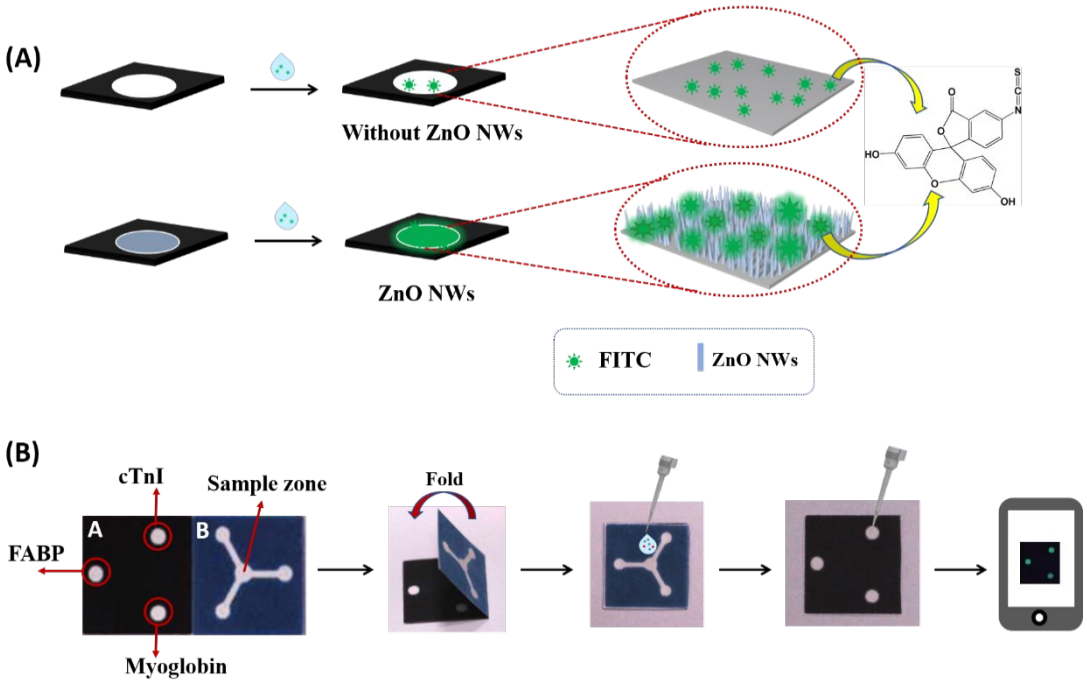

Figure 1. Signal-enhanced detection of multiple cardiac biomarkers by a paper-based fluorogenic immunodevice integrated with ZnO NWs. (A) Schematic illustration showing signal enhancement of the fluorescence intensity by a paper-based device integrated with ZnO NWs. (B) Digital photographs of paper-based devices showing the procedure for multiplexed detection of three cardiac biomarkers, FABP, cTnI, and myoglobin, on a paper-based device, using a smartphone to capture the fluorescence images.

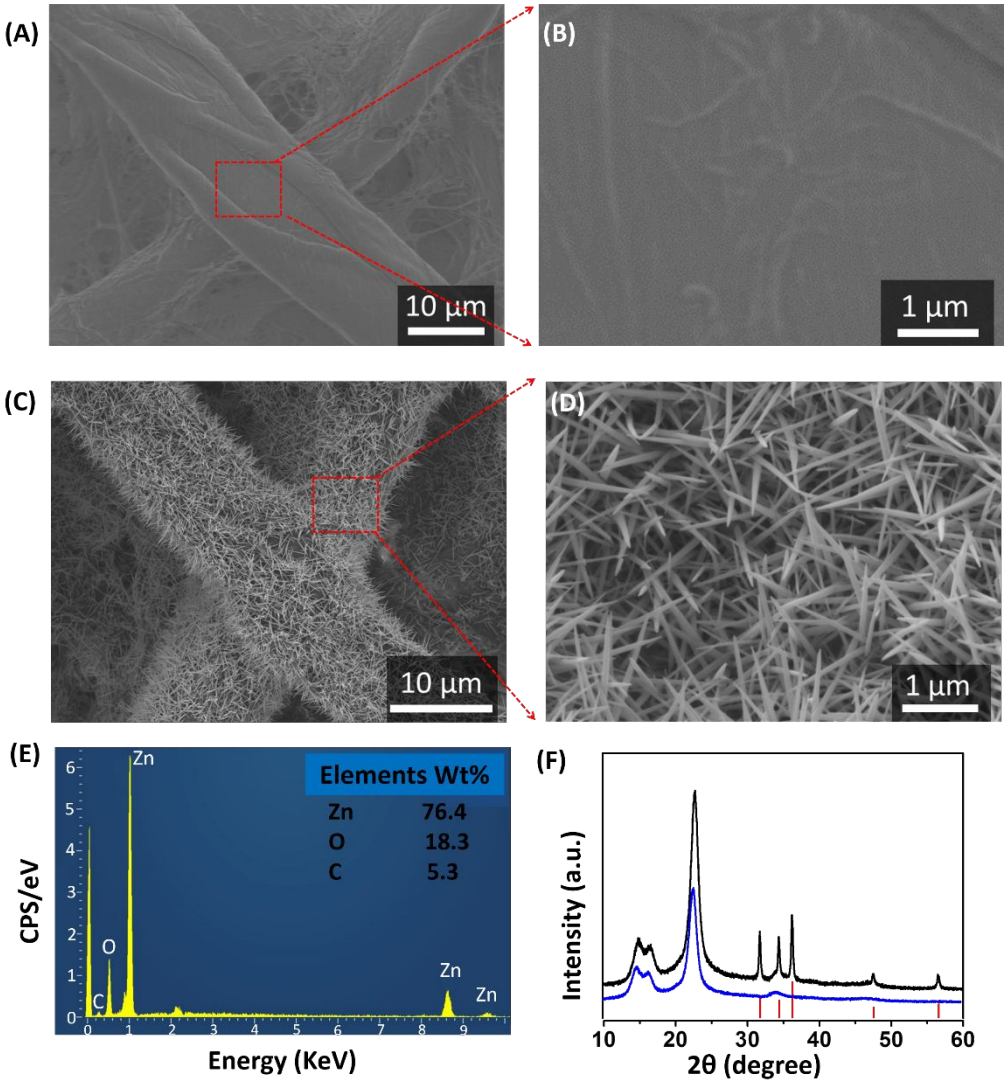

Figure 2. Characterization of ZnO NWs grown on paper. (A) SEM image and (B) enlarged SEM image of paper. (C) SEM image and (D) enlarged SEM image of ZnO NW/paper. (E) EDS spectrum of ZnO NW/paper. CPS: counts per second. (F) XRD patterns of paper (blue line) and ZnO NW/paper (dark line). The red lines inserted are PDF cards of zincite (PDF#36-1451).

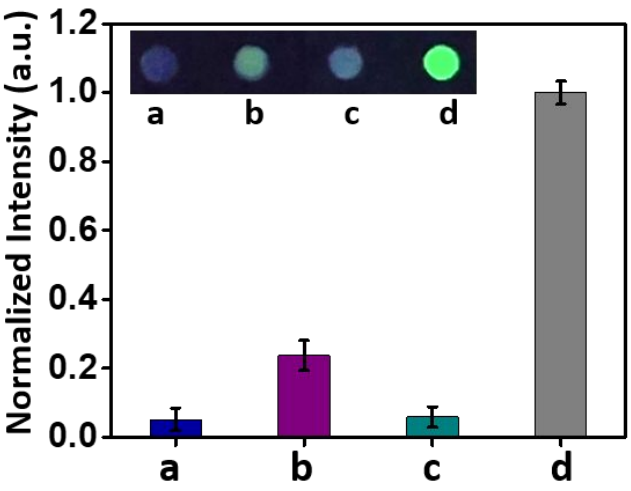

Figure 3. Signal enhancement by ZnO NWs on paper. Histogram of the fluorescence intensity of (a) 2.5 μL of PBS on paper, (b) 2.5 μL of 1 μg/mL FITC-labeled IgG solution on paper, (c) 2.5 μL of PBS on ZnO NW/paper, and (d) 2.5 μL of 1 μg/mL FITC-labeled IgG solution on ZnO NW/paper (Inset: corresponding fluorescence images).

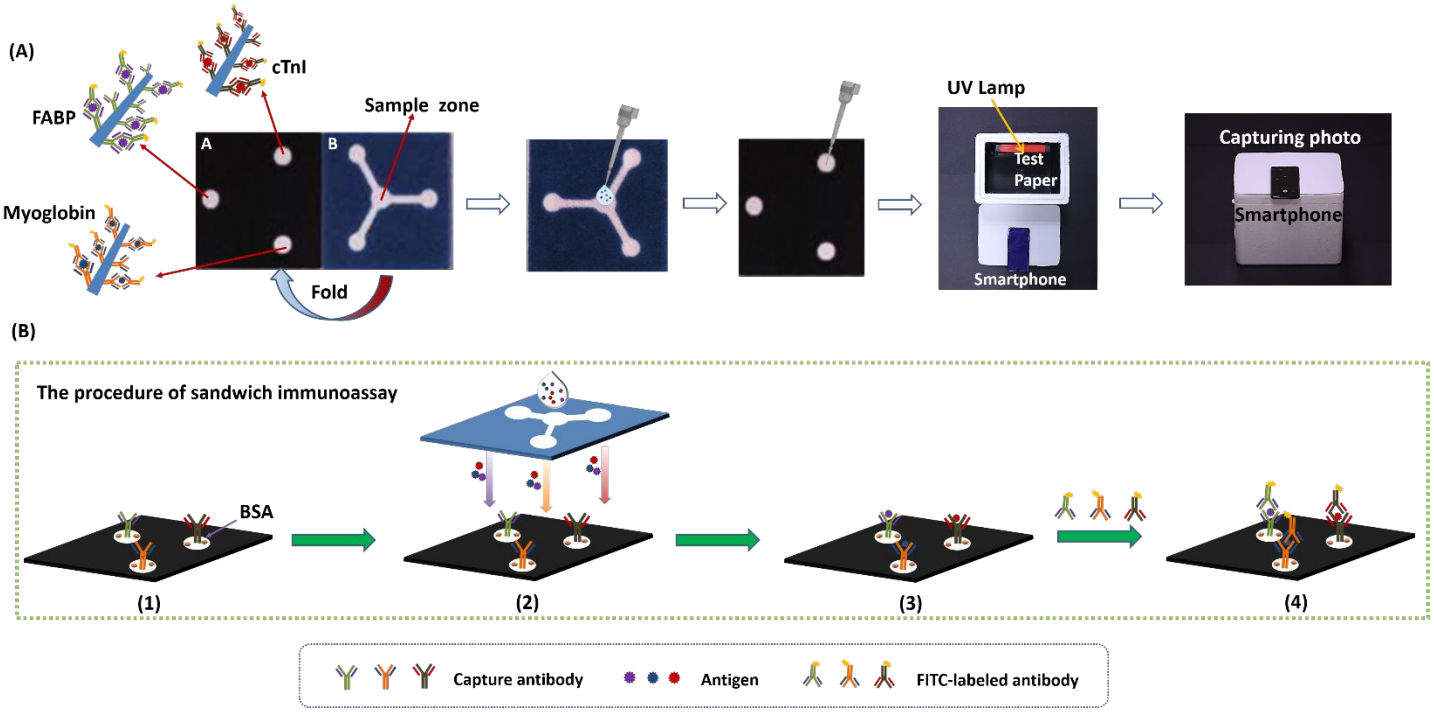

Figure 4. Portable detection of three cardiac biomarkers, FABP, cTnI, and myoglobin, by a sandwich immunoassay on a paper-based device. (A) The paper-based detection was performed in a homemade chamber using a battery-powered UV lamp for excitation and a smartphone for capturing the fluorescence images. (B) The procedure of sandwich immunoassay: (1) Capture antibodies were immobilized on ZnO NW/paper at detection zones. (2) The sample containing cardiac biomarkers was added to the central sample zone. (3) Cardiac biomarkers specifically bound to the respective capture antibodies. (4) The cardiac biomarkers were sandwiched between the capturing antibody and FITC-labeled antibody.

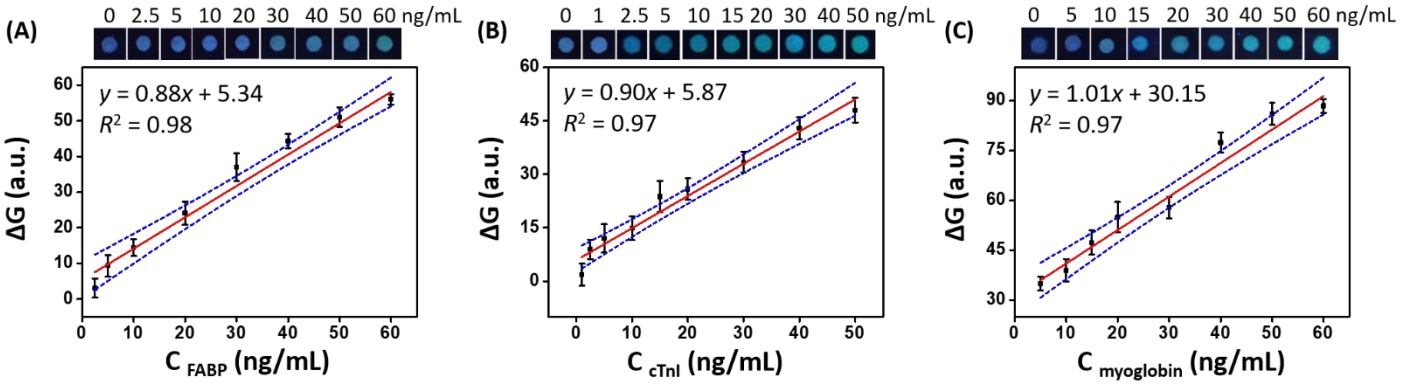

Figure 5. Quantitative detection of three cardiac biomarkers using a paper-based fluorogenic immunodevice integrated with ZnO NWs: (A) FABP, (B) cTnI, and (C) myoglobin. The linear relationship between the G channel intensity and the concentrations of corresponding cardiac biomarkers. Data points for each concentration are the mean of seven replicates, and the background of the paper has been subtracted. Error bars indicate one standard deviation (n = 7), with 95% (blue lines) confidence bands.

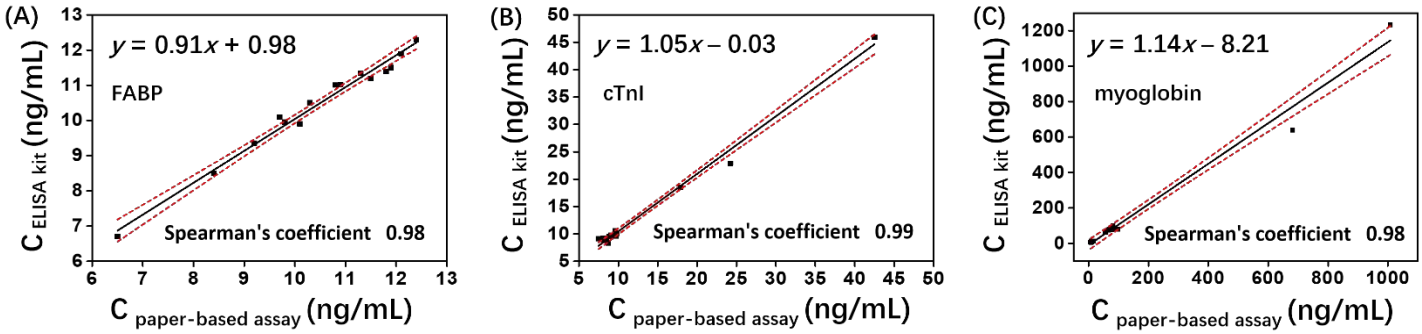

Figure 6. Passing-Boblok regression lines between the results obtained from paper-based devices and commercialized ELISA kits for detection of (A) FABP, (B) cTnI, and (C) myoglobin in clinical samples. The solid dark lines represent the linear regressions, and the red dashed lines show the range of the 95% confidence bands.

Table 1. Assay results for FABP, cTnI, and myoglobin spiked in human serum by a paper-based fluorogenic immunodevice integrated with ZnO NWs (n = 7).

Samples	cTnI concentration (ng/mL)			FABP concentration (ng/mL)			Myoglobin concentration (ng/mL)		
	Added (ng/mL)	Found (ng/mL)	Recovery (%)	Added (ng/mL)	Found (ng/mL)	Recovery (%)	Added (ng/mL)	Found (ng/mL)	Recovery (%)
1	10	9.6	96	10	10.3	103	10	10.04	100.4
2	20	20.4	102	20	20.1	100.5	20	20.02	100.1
3	25	24.9	99.8	25	25.2	100.8	25	25.03	100.12
4	30	30.2	100.6	30	29.9	99.7	30	30.1	100.3

For TOC only: